Remote Sensing Image-Based Analysis of the Impact of Land Use/Land Cover Changes on Land Surface Temperature

Ertie C. Abana, May Z. Valdez, Jeromie S. Salas, Analiza M. Mateo

Abstract*: This study evaluated the land use/land cover (LULC) changes in Tuguegarao City and analyzed its impact on Land Surface Temperature (LST). It was carried out using Remote Sensing and Geographic Information System (GIS) techniques. Three Landsat TM and ETM+ images data were acquired for the years 1990, 2005 and 2016 from USGS Earth Explorer portal. ArcGIS software was used to determine the area statistics of the different land cover and to make the final LULC map. LST for the study area was taken from the thermal infrared band of the satellite images by converting the image digital number into degrees Kelvin using the LMin and LMax spectral radiance scaling factors. The largest areal change appeared in the built-up area with an increase of 1120.32 ha. However, this study detected higher LST in the crop land, grassland and barren land areas of the city rather than the built-up parts of the city which does not follow many of previous studies. The results of the study can be presented to the Local Government Unit so that they can draft appropriate laws for the betterment of the city specially that rapid urbanization and uncontrolled population growth may have extreme impact on the environment.

***Keywords*: Land use/Land cover, Land Surface Temperature, Remote Sensing, Geographical Information System.**

I. INTRODUCTION

Significant changes have occurred in the global environmental system over the last century. Local, regional, and global land surface temperatures have increased ominously [1]. This problem is not only because of greenhouse gasses. A major portion of warming is also due to LULC changes [2]. The drastic change in LULC associated with human activities is regarded as an influential driving force in understanding local climate changes [3], [4].

The 2018 Revision of World Urbanization Prospects produced by the Population Division of the UN Department of Economic and Social Affairs (UN DESA) estimated that more than 50% of the global population lives in urban areas, and this percentage will reach 69.6% by 2050. This projected growth of population in urban areas would mean more urban infrastructure will be put up to meet the needs of the people. However, urban development has major impact on climate change [5], [6]. It harmfully impacts the environment mainly by the proliferation of pollution and the covering of the soil surface with manmade surfaces [1], [2]. This increase in developed land is also continuously decreasing the vegetative cover of the earth's surface and increasing the LST of the urban environment [5], [7].

During the past three decades, the economy of Tuguegarao City, a premiere city in the northeastern Luzon, slowly shifted from farming to manufacturing and commercial economic activities such as trading, advertising, commerce, warehousing, and services which all involve an unusual increase in the population of the city and involves change in the LULC of the city. These changes in LULC may have caused a significant change in the land surface temperature as the very high surface temperature of 42.2 °C was observed twice already in the city on April 22, 1912, and on May 11, 1969, both during the summertime [8]. This very high temperature will continue as Philippine Atmospheric Geophysical and Astronomical Services Administration (PAGASA) observed that temperatures across the country continued to soar as the actual heat index has reached dangerous levels. In fact, PAGASA reported that the climate project for Region 2 is expected to rise by 0.8 °C to 1.0 °C in 2020 and by 1.8 °C to 2.2 °C in 2050.

The high surface temperature that has been recorded in the city and the associated impacts of LULC to land surface temperature discovered in many studies prompted the researchers to evaluate the impact of LULC change to the land surface temperature during summertime in Tuguegarao City. The result of this study would not only help urban planners in identifying areas considered as hotspots and point to them what they need to do to improve the overall living conditions of urban areas but this study would also be beneficial to other cities having similar climate and experiencing similar living conditions.

II. MATERIALS AND METHOD

The study area was the city of Tuguegarao. It is a first-class city in the province of Cagayan, Philippines. It is located along the Cagayan River near the southern border of the province at 17°37′ N and 121°43′ E. The city is located near the mouth of the Pinacanauan River which empties into the Cagayan River. It is surrounded by mountains such as the Sierra Madre Mountains, Cordillera Mountains and the Caraballo Mountains to the east, west, and south, respectively.

Revised Manuscript Received on November 15, 2019

Ertie C. Abana, Center for Engineering Research and Technology Innovation, University of Saint Louis, Tuguegarao City, Cagayan, Philippines. Email: ertie04@gmail.com

May Z. Valdez, Geodetic Engineering Program, University of Saint Louis, Tuguegarao City, Cagayan, Philippines.

Jeromie S. Salas, Geodetic Engineering Program, University of Saint Louis, Tuguegarao City, Cagayan, Philippines.

Analiza M. Mateo, Geodetic Engineering Program, University of Saint Louis, Tuguegarao City, Cagayan, Philippines.

The city covers an approximate area of 114.80 km2 with a population of about 153,502 based on the 2015 Census of Population. It is recognized as the political, economic, and educational center of Cagayan. On average, the temperatures are always high with a mean annual temperature that ranges from 24.5 ºC to 30.5 ºC. The hottest day recorded in the Philippines was in Tuguegarao on May 11, 1969 with a temperature of 42.2 ºC [8]. Thus, analysis and monitoring of land surface temperature are needed in this city.

A. Image Pre-Processing and Classification

The research work was carried out using Remote Sensing and Geographic Information System (GIS) techniques. Due to the limited sources of data, the years were chosen on the basis of the availability of the imageries.

Table- I: Land Cover Classification Scheme

Land Cover	Description
Built-Up Area	Refers to the impervious surface in urban areas including buildings, parking lots and roadways
Crop Land	Defined as arable or cultivable land including both cropped and temporarily plowed land. Cropped land refers to land under annual crops, such as cereals, cotton, wheat and vegetables
Inland Water	Refers to all of the water bodies in the study area, including rivers, lakes, wetlands, fish ponds and other bodies of water
Grassland	Includes residential lawns, parks, golf courses and other areas covered with grass but does not include areas covered by annual crops
Wooded Land	Covered with trees or woods, wooded area near the highway
Barren Land	In general, Barren Land has thin soil, sand, or rocks. Barren lands include deserts, dry salt flats, beaches, sand dunes, exposed rock, strip mines, quarries, and gravel pits.

Three Landsat TM and ETM+ images data acquired in April, for the years 1990, 2005 and 2016 were downloaded from USGS Earth Explorer portal and delivered in GeoTIFF file format. These images had a clear weather condition and had undergone radiometric calibration and atmospheric correction through the software Environment for Visualizing Images (ENVI 5.2). The boundary of Tuguegarao was extracted from the political boundary of Cagayan obtained from Department of Environment and Natural Resources (DENR). GIS software was used to extract the boundary of Tuguegarao City in Landsat images. Both the Landsat TM and ETM+ bands cover the spectral ranges between 0.45–2.5 µm. All of the images were orthorectified and georeferenced to the UTM Luzon 51N map projection prior to the interpretation.

he image classification process is done so that all pixels of a digital image are categorized into themes or one of several land cover classes. A thematic map of the land cover present in an image was produced by using the categorize data [9]. The classification is then performed based on the multispectral data while the numerical basis for categorization is based on the spectral pattern present within the data for each pixel [9]. The land cover maps were created using the band combination of 3, 2, 1 (Landsat TM and ETM+ images) to allow visual interpretation of the images in their natural color. Based on prior knowledge of the land cover from field surveys and previous studies, the classification scheme of the study area shown in Table I was modified in accordance with the land use classification system of the DENR.

Land Use/Land Cover Maps of the study area were generated by supervised classification. Examples of the information classes of interest in the image was identified using supervised classification which is called "training sites". For each information class, a signature analysis was done wherein statistical characterization of the reflectance is developed using the image processing software ArcGIS and then making a decision as to which of the signatures resembles a particular information class. A statistical decision criterion to assist in the classification of overlapping signatures called maximum likelihood classification was utilized in the decision making since it gives more accurate results [10], [11], [12] than other classification algorithms. The image processing software ArcGIS was also used for spatial analyses.

B. Accuracy Assessment and Detection

Accuracy assessment was performed using the following procedure. First, to increase the accuracy of the land cover mapping of the images, ancillary data, Landsat TM and ETM+ images of 1990, 2005 and 2016 were used to collect the reference data. Second, for each classified map, 30 samples for each land-use class were selected using a stratified random method to represent the different land cover classes of the study area. Therefore, 180 samples were used to check the accuracy of the classified maps. Then, the reference data and the results of the visual interpretation were combined with the classification results to improve the classification accuracy of the classified images. The overall accuracy for the 1990, 2005 and 2016 LULC maps was 95.63%, 93.13%, and 99.38%, respectively. These are over the minimum level of interpretation accuracy in the identification of land use and land cover categories from remote sensor data that is at least 85 percent according to [13].

In this study, the area statistics for the different LULC types in the study area among the three observed years were tabulated to clearly see the changes in their area. This study used the ArcGIS software to determine the area statistics of the different land cover and to make the final LULC maps.

C. Derivation of Land Surface Temperature

When using multi-temporal satellite images in quantitative retrieval of LST, it is crucial to eliminate the atmospheric effect by radiometric correction and atmospheric correction [14]. LST for the study area in the epochs of the study was extracted from the thermal infrared band, Band 6, of the satellite images by converting the image Digital Number (DN) into degrees Kelvin using the LMin and LMax (1) spectral radiance scaling factors. This method has been adopted from the USGS Landsat Users handbook. The values used in calculating (1) is in Table II.

$$L\lambda = \left(\frac{LMAX\lambda - LMIN\lambda}{QCALMAX - QCALMIN}\right) * (QCAL - QCALMIN) + LMIN\lambda \quad (1)$$

where:
L_λ = spectral Radiance at the sensor's aperture
QCAL = quantized calibrated pixel value
$LMIN_\lambda$ = spectral radiance that is scaled to QCALMIN

$LMAX_\lambda$ = spectral radiance that is scaled to QCALMAX
QCALMIN = minimum quantized calibrated pixel value
QCALMAX = the maximum quantized calibrated pixel value

Table- II: Spectral Radiance and Quantized Calibrated Pixel Value

Images' Header File (Landsat TM/ETM+)	$LMIN_\lambda$	$LMAX_\lambda$	QCALMIN	QCALMAX
Landsat 5 TM *(April 10,1990)*	1.238	15.303	1	255
Landsat 7 ETM+ (*April 11, 2005, April 9,2016)*	0	17.040	1	255

TM/ETM+ Band 6 imagery was converted from spectral radiance into the effective surface temperatures of the viewed Earth-atmosphere system. This was done under an assumption of unity emissivity and using pre-launch calibration constants. The conversion formula is:

$$T = \frac{K2}{\ln\left(\frac{K1}{L\lambda}+1\right)} \qquad (2)$$

where:
T = Effective surface temperature in Kelvin
K2 = Calibration constant 2 from Table III
K1 = Calibration constant 1 from Table III
L = Spectral radiance

Table- III: Thermal Band Calibration Constants from USGS Landsat Users Handbook

	Constant 1	Constant 2
Landsat 7	666.09	1282.71
Landsat 5	607.76	1260.56

III. RESULTS AND DISCUSSION

A. Patterns of Land Use/Land Cover Changes

Land use and land cover maps of Tuguegarao City during summertime in 1990, 2005 and 2016 which was derived from maximum likelihood supervised classification are shown in Fig. 1, Fig. 2 and Fig. 3, respectively. The total area of every land use category and the percentage of each class between the periods of the study were calculated and are presented in Table IV. The largest area was cropland, followed by grassland, built-up area, barren land, inland water, and wooded land.

Table V represents the area changes in different types of land cover from 1990 to 2016. The largest areal change appeared in the built-up area with an increase of 1120.32 ha (52.86%). This wider variation in urbanized area illustrates that the city experienced rapid urbanization during the past twenty-six years. The dramatic change to the land cover of built-up areas was also evident in previous research findings of different researches from various countries [15], [16], [17]. The area of inland water is fluctuating since the course of rivers was being affected by many factors. Also, seasonal variation in precipitation influences the classification of water bodies. Other small bodies of water were dry at some year, and so these areas were classified into other land cover types. This can explain the water area decrease from 1990 to 2005.

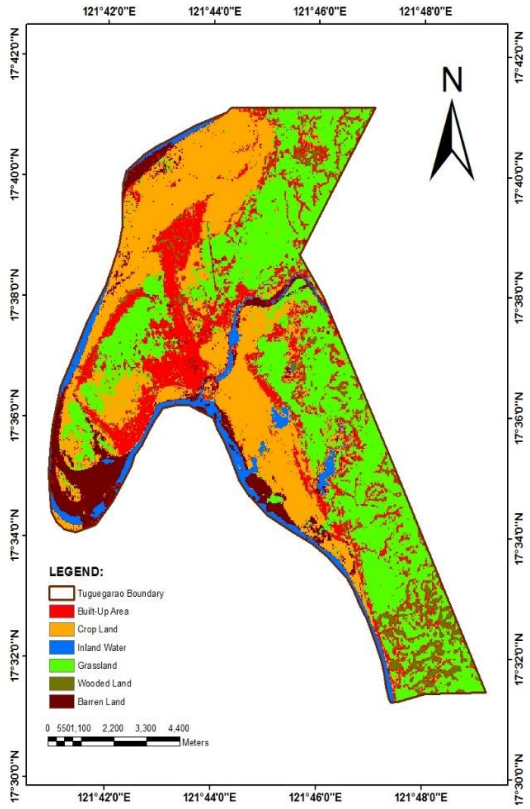

Fig. 1. Land use and land cover maps on April 10, 1990.

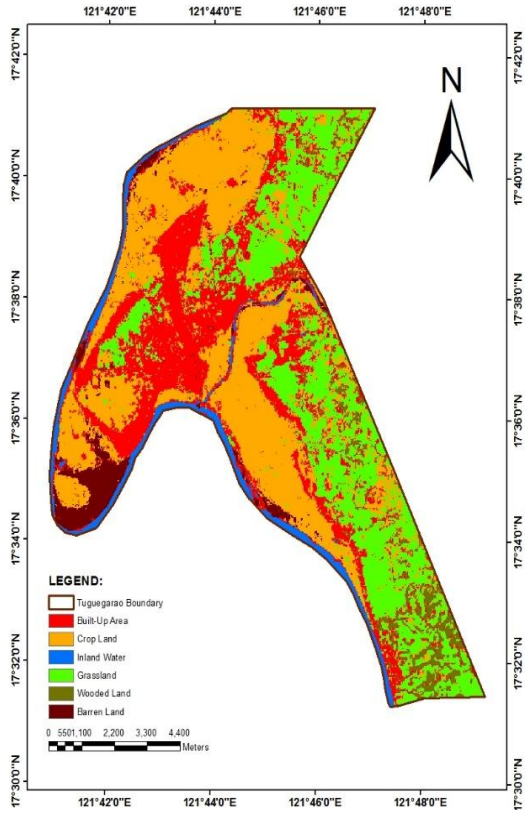

Fig. 2. Land use and land cover maps on April 11, 2005

Table- IV: Area statistics (hectares) for different LULC types in 1990, 2005, and 2016

LULC Types	1990		2005		2016	
	Area	*%*	*Area*	*%*	*Area*	*%*
Built-Up Area	2119.59	18.58	2873.52	25.18	3239.91	28.39
Crop Land	3232.17	28.33	4161.15	36.47	3999.96	35.05
Inland Water	594.45	5.21	528.12	4.63	597.06	5.23
Grassland	4195.35	36.77	2996.64	26.26	2717.01	23.81
Wooded Land	442.08	3.87	385.92	3.38	367.11	3.22
Barren Land	827.28	7.25	465.57	4.08	489.87	4.29

Table- V: Area changes (hectares) of each LULC type among the three observed years

LULC Types	1990-2005		2005-2016		1990-2016	
	Area change	*%*	*Area change*	*%*	*Area change*	*%*
Built-Up Area	753.93	35.57	366.39	12.75	1120.32	52.86
Crop Land	928.98	28.74	-161.19	-3.87	767.79	23.75
Inland Water	-66.33	-11.16	68.94	13.05	2.61	0.44
Grassland	-1198.71	-28.57	-279.63	-9.33	-1478.34	-35.24
Wooded Land	-56.16	-12.70	-18.81	-4.87	-74.97	-16.96
Barren Land	-361.71	-43.72	24.3	5.22	-337.41	-40.79

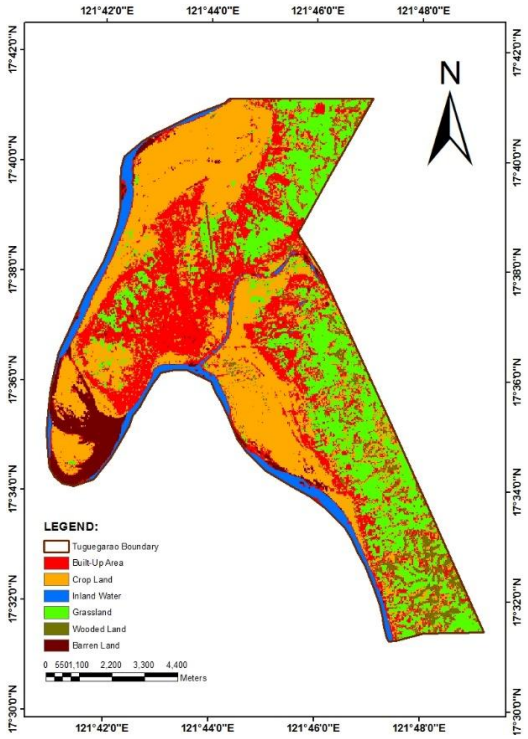

Fig. 3. Land use and land cover maps on April 9, 2016

B. Land Surface Temperature

LST distribution maps were generated for each of the years of study as depicted in Fig. 4, Fig. 5 and Fig. 6. There was an increase in the mean temperatures in 1990, 2005 and 2016. The mean LST values for each type of LULC in 1990, 2005 and 2016 are summarized in Table VI, Table VII and Table VIII, respectively. The detailed information on the LST difference among different land cover types shows an increasing gradation (warming trend) in thermal response from inland water to wooded land, to the built-up area, to crop land, to grassland, and finally to barren land in all epochs of the study. Inland water exhibits the lowest mean temperatures as compared to other land cover types. This is a normal scenario because surface temperatures increase at a greater rate over land than bodies of water [19].

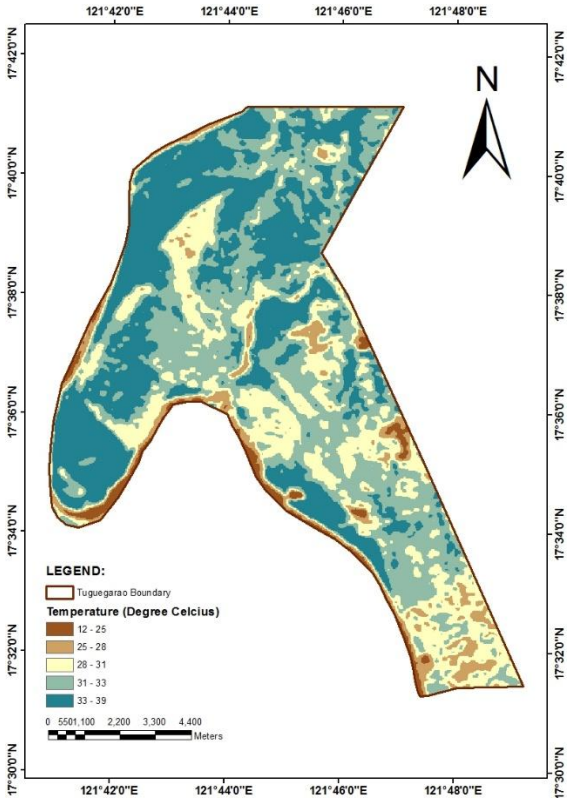

Fig. 4. LST Distribution Map on April 10, 1990

This study detected higher temperatures in the cropland, grassland and barren land areas of the city rather than in the built-up parts of the city. These LST outcomes of this study may disagree with previous studies [1], [20] which show higher LST values in urban areas than in the surrounding area and outside cities. The lower LST in built-up areas compared with the LST in the crop land, in the grassland and in the barren land conform to the study of [21]. This was due to the sun's heat in these areas being absorbed directly into the ground, causing it to heat up faster.

In contrast, roads, pavements, buildings, concrete and other features that make up a built-up area tend to release the absorbed heat slowly.

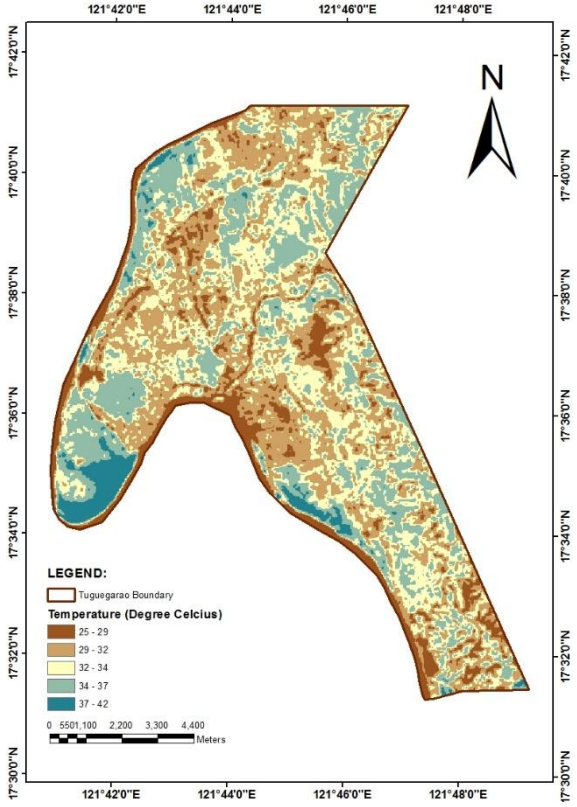

Fig. 5. LST Distribution Map on April 11, 2005

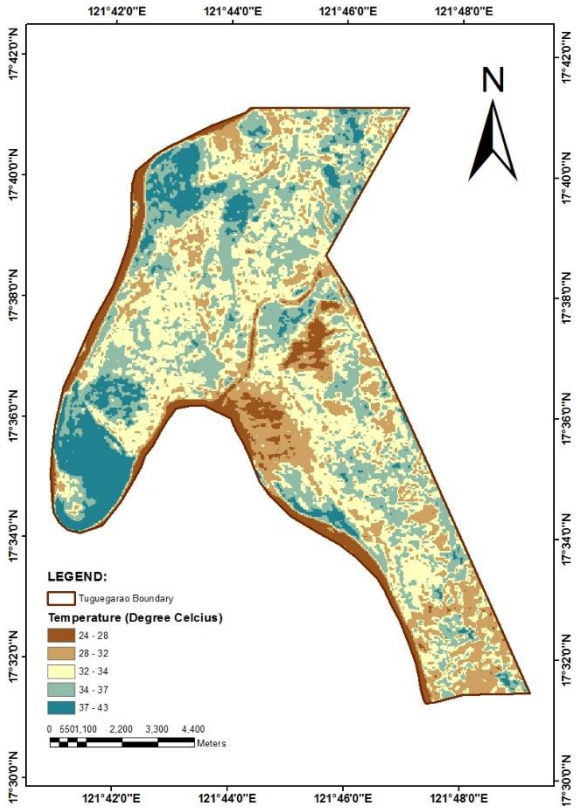

Fig. 6. LST Distribution Map on April 9, 2016

Table- VI: Land Surface Temperatures (°C) for different LULC types on April 10, 1990

LULC Types	Min	Max	Mean	Standard Deviation
Built-up	27.10	33.26	30.23	1.20
Crop Land	27.93	37.61	33.59	1.68
Inland Water	20.62	32.86	25.43	1.84
Grassland	14.71	36.83	33.01	2.27
Wooded land	23.25	31.24	27.15	1.45
Barren land	17.93	38.39	34.95	5.27

Table- VII: Land Surface Temperatures (°C) for different LULC types on April 11, 2005

LULC Types	Min	Max	Mean	Standard Deviation
Built-up	26.36	35.46	30.75	1.56
Crop Land	27.84	38.66	33.12	2.25
Inland Water	25.37	36.84	27.05	1.24
Grassland	29.31	37.30	33.31	1.32
Wooded land	27.35	30.75	28.48	0.67
Barren land	33.13	42.23	39.15	2.21

Table- VIII: Land Surface Temperatures (°C) for different LULC types on April 9, 2016

LULC Types	Min	Max	Mean	Standard Deviation
Built-up	25.36	36.84	32.54	1.85
Crop Land	27.84	39.56	34.64	2.55
Inland Water	24.87	30.75	26.28	1.16
Grassland	28.33	39.11	34.70	1.57
Wooded land	27.84	31.72	29.22	0.82
Barren land	36.84	41.79	40.00	1.16

The statistics of LST for the observed years is shown in Table IX which shows an increasing temperature from the past 26 years. The increase in LST of built-up areas conforms to the finding of [16]. This is because surfaces are now containing concrete and asphalt rather than plants, soil and water resources that contain good absorption and humidity.

Table- VI: Land Surface Temperature increase for the last 26 years

LULC Types	Total Increase (°C)	Yearly Increase (°C)
Built-up	2.31	0.09
Crop Land	1.05	0.04
Inland Water	0.85	0.03
Grassland	1.69	0.07
Wooded land	2.07	0.08
Barren land	5.05	0.19

IV. CONCLUSION

This study revealed the drastic changes in land use/land cover in the study area. Data analysis from 1990 to 2016 showed that there is a noticeable increase in built-up areas and crop land. An obvious decrease in the areas of grassland, wooded land, and barren land was also obtained. For inland water areas, slight increases were computed. The changes in land use/land cover modified the radiant surface temperature and the thermal response of each LULC type that was obtained. However, this study detected higher temperatures in the crop land, grassland and barren land areas of the city rather than the built-up parts of the city. It was also revealed that the land surface temperature has increased in all types of classified LULC in the duration of the study period.

The researchers recommend the densification of the meteorological stations (PAGASA) network and enhancement of their capabilities for climate change monitoring through Remote Sensing techniques. Concerned government agencies should also look into the possibility of establishing true ground control points using GPS to be used as reference points in classifying different LULC types. Moreover, further study can be conducted that considers the vegetation index and its impact on LST. A study that considers the impact of pollution in LST through the use of RS and GIS can also be conducted.

REFERENCES

1. K. S. Kumar, P. U. Bhaskar, and K. Padmakumari, "Estimation of land surface temperature to study urban heat island effect using Landsat ETM+ image," International journal of Engineering Science and technology, 4(2), pp.771-778, 2012.
2. D. E. Comarazamy, J. E. González, J. C. Luvall, D. L. Rickman, and R. D. Bornstein, "Climate impacts of land-cover and land-use changes in tropical islands under conditions of global climate change," Journal of Climate, 26(5), 1535-1550, 2013.
3. A. Karimi, P. Pahlavani, and B. Bigdeli, "Land use analysis on land surface temperature in urban areas using a geographically weighted regression and landsat 8 imagery, a case study: Tehran, Iran, International Archives of the Photogrammetry," Remote Sensing & Spatial Information Sciences, 42, 2017.
4. M. J. Fasona, A. S. Soneye, O. J. Ogunkunle, O. A. Adeaga, O. A. Fashae, and Abbas II, "Simulating Land-Cover and Land-Use Change in the Savanna Under Present Day and Future Climate Scenarios-A GIS-Based Approach," Earth Science Research, 3(1), 25, 2013.
5. E. Igun, & M. Williams, Impact of urban land cover change on land surface temperature, Global Journal of Environmental Science and Management, 4(1), 47-58, 2018.
6. M. E. Kahn, "Urban growth and climate change," Annual Rev. Resour. Econ., 1(1), 333-350, 2009.
7. Y. Kant, B. D. Bharath, J. Mallick, C. Atzberger, and N. Kerle, "Satellite-based analysis of the role of land use/land cover and vegetation density on surface temperature regime of Delhi, India," Journal of the Indian Society of Remote Sensing, 37(2), 201-214, 2009.
8. E. De Vera-Ruiz, "Metro Manilans experience hottest day of the year," Manila Bulletin, 2018.
9. T. Lillesand, R. W. Kiefer, and J. Chipman, "Remote sensing and image interpretation," John Wiley & Sons, 2014.
10. V. Vijaya, and G. J. Niveditha, "Classification of COSMO SkyMed SAR data based on coherence and backscattering coefficient," International Journal Computing Sciences Inf, 1(4), 60-63, 2012.
11. G. S. Korgaonkar & R. R. Sedamkar, "Hyperspectral Image Classification on Decision level fusion," International Conference & Workshop on Recent Trends in Technology (TCET), 1-9, 2012.
12. T. Sarath, G. Nagalakshmi, and S. Jyothi, "A study on hyperspectral remote sensing classifications," International Journal of Computer Applications, 0975-8887, 2014.
13. J. R. Anderson, "A land use and land cover classification system for use with remote sensor data," US Government Printing Office, vol. 964, 1976.
14. K. Themistocleous, D. Hadjimitsis, M. Ioannides, & C. R. I. Clayton, "Integrating satellite remote sensing and spectroradiometric measurements for monitoring archaeological site landscapes," 2008.
15. H. G. Coskun, U. Alganci, and G. Usta, "Analysis of land use change and urbanization in the Kucukcekmece water basin (Istanbul, Turkey) with temporal satellite data using remote sensing and GIS," Sensors, 8(11), 7213-7223, 2008.
16. T. Laosuwan, T. Gomasathit, and T. Rotjanakusol, "Application of Remote Sensing for Temperature Monitoring: The Technique for Land Surface Temperature Analysis," Journal of Ecological Engineering, 18(3), 2017.
17. A. A. Mamun, A. Mahmood, & M. Rahman, "Identification and monitoring the change of land use pattern using remote sensing and GIS: A case study of Dhaka City," IOSR Journal of Mechanical and Civil Engineering, 6(2), 20-28, 2013.
18. R. Alig, S. Stewart, D. Wear, and D. Nowak, "Conversions of forest land: trends, determinants, projections, and policy considerations," Gen. Tech. Rep. PNW-GTR-802. Portland, OR: US Department of Agriculture, Forest Service, Pacific Northwest and Southern Research Stations, 802, 1-26, 2010.
19. M. P. Byrne, and P. A. O'gorman, "Land–ocean warming contrast over a wide range of climates: Convective quasi-equilibrium theory and idealized simulations," Journal of Climate, 26(12), 4000-4016, 2013.
20. J. Rogan, M. Ziemer, D. Martin, S. Ratick, N Cuba, and V. De Lauer, "The impact of tree cover loss on land surface temperature: A case study of central Massachusetts using Landsat Thematic Mapper thermal data," Applied Geography, 45, 49-57, 2013.
21. G. Faqe Ibrahim, "Urban land use land cover changes and their effect on land surface temperature: Case study using Dohuk City in the Kurdistan Region of Iraq," Climate, 5(1), 13, 2017.

AUTHORS PROFILE

Ertie C. Abana received BS in Computer Engineering and Master of Information Technology degrees from the University of Saint Louis in 2011 and 2016, respectively, and is working for his PhD degree. He is a faculty of the School of Engineering, Architecture, and Information Technology Education, University of Saint Louis, Tuguegarao City, Philippines since 2014. He has published papers in the areas of embedded systems, microcontrollers, fuzzy systems, data mining, and software usability.

May Z. Valdez received BS in Geodetic Engineering and Master in Engineering Major in Geodetic Engineering degrees from the University of Saint Louis. He is the program coordinator of Geodetic Engineering Program of the School of Engineering, Architecture, and Information Technology Education, University of Saint Louis, Tuguegarao City, Philippines. Her research interests are in the areas of GIS applications, remote sensing, land-use and land-cover assessment, and land suitability analysis.

Jeromie S. Salas received BS in Geodetic Engineering from the University of Saint Louis, Tuguegarao City, Philippines. His research interests are in the areas of GIS applications, remote sensing, and land-use and land-cover assessment.

Analiza M. Mateo received BS in Geodetic Engineering from the University of Saint Louis, Tuguegarao City, Philippines in 2019. His research interests are in the areas of GIS applications, remote sensing, and land-use and land-cover assessment.